Microwave Spectrum and Structure of the Pyridine-Sulfur Dioxide Complex

Jung Jin Oh, Kurt W. Hillig II, and Robert L. Kuczkowski*

Contribution from the Department of Chemistry, University of Michigan, Ann Arbor, Michigan 48109-1055. *Received March 28, 1991*

Abstract: The rotational spectrum of the charge-transfer complex between pyridine and sulfur dioxide has been studied by using a Fourier transform microwave spectrometer employing a Fabry-Perot cavity and pulsed supersonic nozzle as a molecular beam source. The spectroscopic constants (MHz) for pyridine·SO_2 are A = 3534.946 (4), B = 759.923 (1), C = 647.636 (1), χ_{aa} = -4.087 (3), χ_{bb} = 1.347 (2), and χ_{cc} = 2.740 (2). In addition to the normal isotopic form, the rotational spectra of the $C_5H_5N\cdot{}^{34}SO_2$, $C_5H_5N\cdot S^{18}O_2$, $C_5D_5N\cdot SO_2$, and $C_5H_5{}^{15}N\cdot SO_2$ isotopic species were assigned. Stark effect measurements gave electric dipole components of μ_a = 4.360 (5), μ_c = 1.311 (3), and μ_{total} = 4.552 (5) D. The dipole moment and moment of inertia data show that the complex belongs to the C_s point group. The nitrogen to sulfur distance is 2.61 (3) Å, with the C_2 axis of the pyridine ring approximately perpendicular to the sulfur dioxide plane. The pyridine plane is rotated 90° to the C_2 axis of the SO_2; i.e., the complex is approximately L-shaped. Comparisons are made to the trimethylamine·SO_2, dimethylamine·SO_2, and HCN·SO_2 complexes.

Introduction

The complexes of SO_2 with trimethylamine (TMA),[1] dimethylamine (DMA),[2] and HCN[3] have been investigated recently by high-resolution spectroscopic techniques. In all three cases, the nitrogen lone pair is directed roughly perpendicular to the plane of SO_2 at the sulfur end, suggestive of a n-π^* charge-transfer interaction. The association with the amines is relatively strong, resulting in N···S distances of 2.26 (2) Å in TMA·SO_2 and 2.34 (3) Å in DMA·SO_2. The HCN complex is much weaker with a d(N···S) of 2.98 (1) Å. The interaction distance obviously appears sensitive to the nitrogen basicity. In aqueous solutions, aromatic N-heterocycles are usually not as basic as aliphatic amines. Nevertheless, their interaction with the surroundings is of some interest in biological systems, so it seemed worthwhile to extend these structural studies to a complex between SO_2 and a member of this class. The pyridine·SO_2 (Py·SO_2) complex was an obvious choice.

The Py·SO_2 complex is also of interest because of its chemical importance. It has attracted attention because of its participation in the Karl-Fischer reaction for titrating water in many materials.[4] It is now known that SO_2 is the chemically reactive moiety toward water while the pyridine is a suitable base for controlling the pH of the medium. Solutions of SO_2 in pyridine have also been investigated for use in the Li·SO_2 high-density battery;[5] pyridine is an excellent solvent for this system. In another application, it was found that the Py·SO_2 complex initiates the photopolymerization of methyl methacrylate (MMA) in bulk at 40 °C.[6] The effective initiating species is the SO_2-monomer complex.

The Py·SO_2 complex (mp = -7.0 °C) has been known for some time.[7] Its dissociation constant in solution at room temperature was roughly a factor of 1000 larger than the more stable TMA·SO_2 complex.[7,8] The enthalpy of solution of SO_2 in pyridine has been estimated as -11.6 kcal/mol.[9] This can be compared to -15.0 kcal/mol in dimethylaniline, -6.3 kcal/mol in H_2O, and -3.8 kcal/mol in heptane.[9] The Raman spectrum of this complex dissolved in CCl_4 solution showed a behavior similar to that of the TMA·SO_2 complex: The ν_1 and ν_3 bands of SO_2 were red-shifted, while the ν_2 band was blue-shifted.[10] A preliminary report of the microwave spectrum of this complex showed that the moment of inertia data could fit two distinct structures having a N···S interaction, differing only in the orientation of the pyridine.[11] Additional isotopic data that solve this ambiguity are reported in this paper. Ab initio and distributed multipole electrostatic calculations that shed light on the interactions are also reported.

Experimental Section

Materials. A mixture of 0.5% of pyridine (Aldrich Chemical Co.) and 0.5% of SO_2 (Matheson Co.) seeded in Ar carrier gas at a total pressure of 1-2 atm was used to form the complex in a molecular beam using a supersonic expansion. The $C_5H_5{}^{15}N$ (98% ^{15}N, MSD Isotopes) and C_5D_5N (98% D, Aldrich) species were used without dilution. Enriched $S^{18}O_2$ (99% ^{18}O, Alpha Organic) was used to prepare pyridine·$S^{18}O_2$. The spectrum of the ^{34}S isotopic species was observed in its natural abundance of 4%.

Spectrometer. A Fourier transform microwave spectrometer[12] that operated in the region of 6.9-18 GHz was employed. The system has been described previously.[13] A modified Bosch fuel injector pulsed nozzle was used with a repetition rate of about 23 Hz. The nozzle orifices were 0.5 or 1.0 mm. Timing of the gas and microwave pulses was coordinated to minimize Doppler splitting of the transitions. Typical line widths of ~20 kHz (fwhm) were observed except for some transitions where hyperfine splittings appeared to complicate and broaden the line shape. Center frequencies were usually reproducible to ±1 kHz, and accuracies are estimated to be ±2 kHz.

Spectra. After spectra for various possible structures were predicted, a search located a set of transitions with hyperfine splittings arising from ^{14}N-nuclear quadrupole coupling, which aided in the assignment of rotational quantum numbers. Twenty-nine a-dipole and 12 c-dipole transitions were assigned. Spectroscopic constants were initially determined from a rough estimate of the unsplit frequencies. The analysis of the nuclear hyperfine structure followed based on this first set of rotational constants. The observed transitions were fit by using the familiar treatment of nuclear quadrupole coupling in first order. A proper choice of the hyperfine components and a least-squares fit of all the observed transitions gave the unsplit frequency and the quadrupole coupling constants. The calculated unsplit frequencies were then used to determine the spectroscopic constants with a Watson S-reduced Hamiltonian (I^r representation).[14] Five P^4 centrifugal distortion constants and two P^6 distortion constants were included in the fit. A set of hyperfine split

(1) Oh, J.-J.; LaBarge, M. S.; Matos, J.; Kampf, J. W.; Hillig, K. W., II; Kuczkowski, R. L. *J. Am. Chem. Soc.* **1991**, *113*, 4732.
(2) Oh, J.-J.; Hillig, K. W., II; Kuczkowski, R. L. *J. Phys. Chem.*, in press.
(3) Goodwin, E. J.; Legon, A. C. *J. Chem. Phys.* **1986**, *85*, 6828.
(4) Scholz, E. *Karl Fischer Titration*; Springer-Verlag: New York, 1984.
(5) Moshtev, R. V.; Zlatilova, P. *Electrochim. Acta* **1982**, *27*, 1107.
(6) (a) Ghosh, P.; Chakraborty, S. *Eur. Polym. J.* **1979**, *15*, 137. (b) Ghosh, P.; Biswas, S. *Makromol. Chem.* **1981**, *182*, 1985.
(7) Moede, J. A.; Curran, C. *J. Am. Chem. Soc.* **1949**, *71*, 852.
(8) Grundnes, J.; Christian, S. D. *J. Am. Chem. Soc.* **1968**, *90*, 2239.
(9) (a) Gardner, C. L.; Day, R. W. *Can. J. Chem.* **1984**, *62*, 986. (b) Benoit, R. L.; Milanova, E. *Can. J. Chem.* **1979**, *57*, 1319.
(10) (a) Pawelka, Z.; Maes, G.; Zeegers-Huyskens, Th. *J. Phys. Chem.* **1981**, *85*, 3431. (b) Sass, C. S.; Ault, B. S. *J. Phys. Chem.* **1984**, *88*, 432.
(11) LaBarge, M. S.; Oh, J.-J.; Hillig, K. H., II; Kuczkowski, R. L. *Chem. Phys. Lett.* **1989**, *159*, 559.
(12) Balle, T. J.; Flygare, W. H. *Rev. Sci. Instrum.* **1981**, *52*, 33.
(13) (a) Bohn, R. K.; Hillig, K. W., II; Kuczkowski, R. L. *J. Phys. Chem.* **1989**, *93*, 3456. (b) Hillig, K. W., II; Matos, J.; Scioly, A.; Kuczkowski, R. L. *Chem. Phys. Lett.* **1987**, *133*, 359.
(14) Watson, J. K. G. *J. Chem. Phys.* **1967**, *46*, 1935.

0002-7863/91/1513-7480$02.50/0

Table I. Selected Transition Frequencies for $C_5H_5N{\cdot}SO_2$

transition	F'	F	ν_{obs}[a]	$\Delta\nu$[b]	transition	F'	F	ν_{obs}[a]	$\Delta\nu$[b]
$2_{20}-1_{10}$			11 255.436	0	$4_{23}-3_{13}$			14 457.573	0
	3	2	11 255.281	1		3	2	14 457.113	1
	2	1	11 255.778	−1		5	4	14 457.408	0
$2_{21}-1_{11}$			11 364.386	3		4	3	14 458.104	−1
	1	0	11 364.036	−2	$4_{13}-3_{03}$			9 029.609	0
	3	2	11 364.161	1		3	2	9 029.279	1
	2	1	11 364.074	3		5	4	9 029.517	−1
$2_{20}-2_{12}$			8 665.066	3		4	3	9 029.947	0
	3	3	8 664.578	1	$5_{14}-4_{04}$			10 735.278	−2
	2	2	8 666.778	−1		4	3	10 735.030	−1
$2_{21}-2_{11}$			8 324.868	−4		6	5	10 735.187	1
	3	3	8 324.481	1		5	4	10 735.573	0
	2	2	8 326.225	−1	$5_{05}-4_{04}$			6 971.721	0
$3_{21}-2_{11}$			12 563.145	−2		4	3	6 971.682	1
	2	1	12 562.795	−1		6	5	6 971.747	−1
	4	3	12 563.044	1	$6_{06}-5_{05}$			8 331.317	6
	3	2	12 563.497	0		5	4	8 331.296	0
$3_{22}-2_{12}$			12 883.324	−2	$6_{16}-5_{15}$			8 082.780	1
	2	1	12 882.641	2		6	5	8 082.746	−1
	3	3	12 883.129	1		7	6	8 082.811	1
	4	3	12 883.129	1	$6_{15}-5_{14}$			8 752.864	6
	2	2	12 884.008	−1		6	5	8 752.830	0
	3	2	12 884.008	−1	$6_{25}-5_{24}$			8 427.958	0
$3_{12}-2_{02}$			7 391.416	1		6	5	8 427.837	−1
	2	1	7 390.860	−3		7	6	8 428.016	1
	4	3	7 391.323	3	$6_{24}-5_{23}$			8 541.680	−1
	3	2	7 391.851	1		6	5	8 541.579	1
$3_{22}-3_{12}$			8 157.780	1		7	6	8 541.728	−2
	3	2	8 157.304	−1		5	4	8 541.728	0
	2	2	8 157.304	−1	$6_{34}-5_{33}$			8 456.685	−1
	3	4	8 157.580	−2		6	5	8 456.424	−1
	4	4	8 157.580	−2		7	6	8 456.792	1
	3	3	8 158.376	2		5	4	8 456.848	0
	4	3	8 158.376	2	$6_{33}-5_{32}$			8 460.152	3
	2	3	8 158.376	2		6	5	8 459.895	3
$3_{21}-3_{13}$			8 848.084	3		7	6	8 460.253	2
	2	2	8 847.316	−1		5	4	8 460.309	−5
	4	4	8 847.765	1					
	3	3	8 849.042	0					

[a] Observed frequency (ν_{obs}, MHz). The first frequency listed for each transition is ν_0, the center frequency in the absence of hyperfine splitting. [b] Observed − calculated frequency (kHz) using A, B, C, D_J, etc. in Table II to calculate the center frequency and the quadrupole coupling constants for the hyperfine components.

Table II. Spectroscopic Constants for the Isotopic Species of $C_5H_5N{\cdot}SO_2$

	normal	^{34}S	$^{18}O_2$	^{15}N	D_5
no. of lines[a]	41 (117)	8 (16)	12 (25)	22	10 (17)
A (MHz)	3534.946 (4)	3529.03 (27)	3377.648 (2)	3533.264 (1)	3140.30 (45)
B (MHz)	759.923 (1)	749.534 (6)	736.752 (1)	759.831 (1)	720.378 (9)
C (MHz)	647.636 (1)	640.211 (4)	627.099 (2)	647.611 (1)	606.246 (8)
D_J (kHz)	0.31 (1)	0.36 (2)	0.32 (1)	0.31 (1)	0.12 (3)
D_{JK} (kHz)	41.0 (1)	39.3 (3)	34.9 (1)	41.1 (1)	85.6 (7)
D_K (kHz)	−39.4 (9)	−39.4[c]	−39.4[c]	−39.4[c]	−39.4[c]
d_1 (kHz)	−0.103 (3)	−0.180 (30)	−0.115 (5)	−0.110 (1)	−0.24 (5)
d_2 (kHz)	−0.012 (2)	−0.031 (6)	0.008 (5)	0.009 (1)	−0.21 (2)
H_{JK} (kHz)	−0.012 (1)	−0.012[c]	−0.012[c]	−0.012[c]	−0.012[c]
H_{KJ} (kHz)	−0.574 (9)	−0.574[c]	−0.574[c]	−0.574[c]	−0.574[c]
$\Delta\nu_{rms}$ (kHz)[b]	4.5	5.3	5.7	2.1	17.3
χ_{aa} (MHz)	−4.087 (3)	−3.97 (5)	−4.07 (2)		−4.06 (2)
χ_{bb} (MHz)	1.347 (2)	1.38 (8)	1.34 (1)		1.39 (5)

[a] Number in parenthesis is the number of measured quadrupole components. [b] $\Delta\nu = \nu_{obs} - \nu_{calc}$. [c] Fixed to the value for the normal isotope.

transitions are listed in Table I. The complete set is available as supplementary material (Table S1). The derived spectroscopic constants are given in Table II.

The assignment of the $C_5H_5{}^{15}N{\cdot}SO_2$, $C_5D_5N{\cdot}SO_2$, $C_5H_5N{\cdot}S^{18}O_2$, and $C_5H_5N{\cdot}{}^{34}SO_2$ species proceeded in a similar manner. For the ^{15}N-enriched species, quadrupole splitting was absent and Stark splittings were used to confirm the assignment. For the other species, the hyperfine patterns were helpful in assigning the transitions. The spectral constants obtained from fitting these transitions are given in Table II. The transitions are available as supplementary material (Tables S2–S5).

Results

Structure. The structure can be derived from the moments of inertia $I_a = \sum_i m_i(b_i^2 + c_i^2)$, etc.,[15] or the related planar moments of inertia $P_{bb} = (I_a + I_c - I_b)/2 = \sum_i m_i b_i^2$, etc. The large values for I_b and I_c eliminated models in which SO_2 and pyridine were parallel and stacked, as in the π–π^* complex of benzene·SO_2,[11] since the short center of mass separation in these models would result in much smaller values than observed (lower by 100–150 amu·Å^2). Rotating the pyridine approximately 90° so that its C_2 axis is nearly perpendicular to the SO_2, and separating their centers of mass by plausible amounts, can sufficiently increase I_b and I_c to match the observed values.

(15) The I's are determined from the spectroscopic constants; for example, $I_a = h/(8\pi^2 A)$. The conversion factor $h/(8\pi^2) = 505\,379.05$ amu·Å^2·MHz was used.

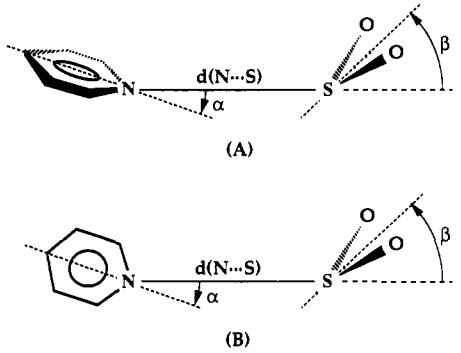

Figure 1. Definition of structural parameters used to describe the L-shaped (A, experimental) and staggered conformations (B) of the pyridine·SO_2 complex.

Table III. Comparison of the Out of Plane Second Moments for $C_5H_5N{\cdot}SO_2$

	P_{bb}[a]	P_{bb}[b]	ΔP_{bb}[c]
$C_5H_5N{\cdot}SO_2$	129.136	132.237	−3.101
$C_5H_5N{\cdot}^{34}SO_2$	129.192	132.237	−3.045
$C_5H_5{}^{15}N{\cdot}SO_2$	129.144	132.237	−3.093
$C_5H_5N{\cdot}S^{18}O_2$	134.785	138.350	−3.565
$C_5D_5N{\cdot}SO_2$	146.503	149.979	−3.476

[a] Observed P_{bb} (amu·Å²). [b] Calculated P_{bb} (amu·Å²) holding pyridine[18] and SO_2[19] geometries fixed in the configuration of Figure 1A. [c] Observed − calculated (amu·Å²).

Table IV. Structural Parameters for Pyridine·SO_2

	I[a]	II[b]	III[c]
R_{cm} (Å)[d]	4.008 (3)	4.015 (1)	4.01 (5)
d(N···S) (Å)[e]	2.601 (3)	2.618 (1)	2.61 (5)
α (deg)[e]	14.0 (1.5)	16.3 (2)	15.1 (50)
β (deg)[e]	81.2 (14.1)	80.4 (2.2)	80.8 (50)
Δ_{rms} (amu·Å²)[f]	2.39	0.27	

[a] Least-squares fit of moments of inertia of all isotopic data holding pyridine and SO_2 geometries fixed.[18,19] [b] Least-squares fit of P_{aa} and P_{cc} holding pyridine and SO_2 geometries fixed. P_{bb} has been ignored. [c] Average of I and II, preferred values. [d] Distance between the centers of mass of pyridine and SO_2. [e] See Figure 1 for definition. [f] $\Delta = I_x$(obs) − I_x(calc) for I and P_x(obs) − P_x(calc) for II.

The a- and c-type selection rules suggest an ac symmetry plane, i.e., structures with C_s symmetry. This requires that the C_2 axes of pyridine and SO_2 lie in the symmetry plane. Models in which the pyridine completely lies in the symmetry plane (Figure 1B) should give a- and b-type spectra and can thus be eliminated. Only structures in which both pyridine and SO_2 straddle the symmetry plane (Figure 1A) are consistent with both the moments of inertia and the selection rules. The P_{bb} planar moments, calculated from the rigid structures of the monomers for this model, are in basic agreement with the observed values, as shown in Table III. Nevertheless, the differences (ΔP_{bb}) are quite large compared to many other complexes.[16] These differences arise from the low-frequency, large-amplitude vibrations in weak complexes. Given the heavy masses of the monomers, an out of plane torsional vibration amplitude of 10–15° can easily cause a large deviation.[17]

To determine the structure of the complex, an ac symmetry plane was assumed and the geometries of Py[18] and SO_2[19] were fixed to their monomer values. This leaves three parameters to define the geometry of the complex. For fitting purposes, these were the center of mass distance R_{cm}, and the two tilt angles of the C_2 axes of the monomers with respect to R_{cm}. However, it is more convenient to compare the intermolecular nitrogen–sulfur distance d(N···S), and the angles α and β between d(N···S) and the C_2 axes of the pyridine and SO_2 as shown in Figure 1A. Two different sets of inertial data were used to determine the structure of the complex. In fit I, the observed moments of inertia of the five isotopic species were least-squares fitted to determine the three structural parameters, while in fit II, P_{bb} was ignored and only the P_{aa} and P_{cc} values were used. The fitted and derived structural parameters based on the above two structural calculations are listed in Table IV and show small differences between them.

Table V. Heavy Atom Coordinates for $C_5H_5N{\cdot}SO_2$ (Å) from Isotopic Data

	|a|		|b|		|c|	
	Kr[a]	I[a]	Kr	I	Kr	I
S	2.140	2.168	0.136[b]	0.0	0.324	0.291
O	2.258	2.260	1.187	1.235	0.517	0.426
N	0.147	0.432	0.094[b]	0.0	0.245	0.356

[a] Coordinate from Kraitchman (Kr) substitution method or least-squares fitting of moments of inertia (I). [b] These values are nonzero because of large amplitude vibrational effects that contaminate the moments of inertia.

Table VI. Comparison of Properties of SO_2 Complexes

	TMA·SO_2[a]	DMA·SO_2[b]	Py·SO_2	HCN·SO_2[c]
d(N···S) (Å)	2.26 (3)	2.34 (1)	2.61 (5)	2.98
α (deg)[d]	0.8 (10)	3.4 (30)	15.0 (50)	23
β (deg)[d]	78.5 (20)	78.7 (30)	80.9 (50)	71
μ_{obs} (D)	4.80 (1)	4.34 (1)	4.82 (2)	
μ_{ind} (D)[e]	2.96	2.78	2.33	
$\Delta\chi_{aa}$ (MHz)[f]	−1.71	−1.08	−0.34	0.17
k_s (mdyn·Å⁻¹)[g]	0.328	0.211	0.084	0.024
ω_s (cm⁻¹)	134.5	116.3	64	46.5
$\langle\Delta R_2^2\rangle^{1/2}$ (Å)	0.064	0.074	0.087	0.138
ϵ (kcal·mol⁻¹)[h]	4.9	3.7	2.7	0.65
ΔE_{diss} (kcal·mol⁻¹)[i]	17.2	16.8	10.1	3.5[j]
IP (kcal·mol⁻¹)[k]	8.44	8.97	9.60	13.60
ΔE_{PA} (kcal·mol⁻¹)[l]	−222.1	−217.9	−218.1	−175.9

[a] Reference 1. [b] Reference 2. [c] Reference 3. [d] See Figure 1 for definition of α and β. [e] $\mu_{obs} - \mu_{calc} = \mu_{ind}$. See discussion. [f] $\Delta\chi_{aa} = \Delta\chi_{aa}{}^{obs} - \Delta\chi_{aa}{}^{calc}$. See Discussion. [g] k_s, ω_s, and ΔR_s are vibrational parameters for the stretching mode along the R_{cm} coordinate. [h] Well depth from k_s for LJ 6–12 potential. See Discussion. [i] Ab initio dissociation energy (HF/3-21G*) for the observed structure; the measured value for TMA·SO_2 is 9.1 kcal/mol.[8] [j] Ab initio, HF/6-31G*.[29] [k] Experimental ionization potential of the nitrogen species.[39] [l] Experimental proton affinity of the nitrogen species.[40]

The Kraitchman substitution coordinates are compared[20,21] in Table V to the values from the least-squares fit. The discrepancies for the small coordinates, especially for the nitrogen, which is very close to the center of mass of the complex, arise from the neglect of the large amplitude vibrational effects. These coordinates were used to determine the sign of the tilt angles α and β, since fitting the moments of inertia data is ambiguous regarding their signs and leads to four different sets of angles. In particular, the negative α gives a c coordinate for the oxygens of 0.28 Å, quite far from the Kraitchman value of 0.52 Å, while the positive sign gives 0.43 Å and is preferred. The reported structure is also consistent with the observed large induced dipole moment (see below), which is

(16) (a) As a comparison, the analogous differences for the HF·SO_2 and HCl·SO_2 complexes are 1.40 and 2.75 amu·Å², respectively.[16b,c] (b) Fillery-Travis, A. J.; Legon, A. C. *Chem. Phys. Lett.* **1986**, *123*, 4. (c) Fillery-Travis, A. J.; Legon, A. C. *J. Chem. Phys.* **1986**, *85*, 3180.

(17) It is not possible to account for the discrepancies in ΔP_{bb} without a detailed knowledge of the elusive vibrational potential function for the complex. However, a crude mechanical model in which the pyridine and/or SO_2 torsionally oscillate about their C_2 axes would reduce the b-coordinates of the out of plane atoms, on average, consistent with the observed values of ΔP_{bb}. The fact that the deviation in ΔP_{bb} is larger for the heavier isotopes (C_5D_5N and $S^{18}O_2$) suggests that such an out of plane motion is strongly coupled to another vibration. A coupling to the van der Waals stretching mode could account for the observed results.

(18) (a) Mata, F.; Quintana, M. H.; Sørenson, G. O. *J. Mol. Struct.* **1977**, *42*, 1. (b) Sørenson, G. O.; Mahler, L.; Rastrup-Andersen, N. *J. Mol. Struct.* **1974**, *20*, 119.

(19) Harmony, M. D.; Laurie, V. W.; Kuczkowski, R. L.; Schwendeman, R. H.; Ramsay, D. A.; Lovas, F. J.; Lafferty, W. J.; Maki, A. G. *J. Phys. Chem. Ref. Data* **1979**, *8*, 619.

(20) Kraitchman, J. *Am. J. Phys.* **1953**, *21*, 17.

(21) Chutjian, A. *J. Mol. Spectrosc.* **1964**, *63*, 1477.

nearly aligned with d(N···S), similar to the TMA·SO_2 and DMA·SO_2 complexes.

The parameters in Table IV are the so-called r_0 structural parameters. For comparison with other species, the average of I and II seems preferable (structure III). It is unclear how much the r_e structural parameters will differ from these values, but estimates of ±0.05 Å in d(N···S) and ±5° in α and β seem plausible. These estimates are the origin of the uncertainties listed in Table IV.

Dipole Moment. The Stark effect of Py·SO_2 was measured by a previously described method.[1] OCS was used as a field calibrant.[22] Transitions of the $C_5H_5{}^{15}N{\cdot}SO_2$ species were employed since complications from quadrupole splittings were absent for this species. The second-order Stark effects ($\Delta\nu/E^2$) for seven M_J components of two transitions of the $C_5H_5{}^{15}N{\cdot}SO_2$ species were determined and are listed in Table S6. A least-squares fit of $\Delta\nu/E^2$ using the calculated second-order coefficients gave dipole components of μ_a = 4.379 (12), μ_c = 1.329 (11), and μ_{total} = 4.576 (12) D, with the $\mu_b{}^2$ component equal to −0.08 D^2. The small negative value for $\mu_b{}^2$ implied that this component was zero, which was expected for a complex with C_s symmetry (see the structure section). When $\mu_b{}^2$ was fixed to zero, the least-squares fit gave μ_a = 4.360 (5), μ_c = 1.311 (3), and μ_{total} = 4.552 (5) D.

Discussion

It is interesting to compare the results for Py·SO_2 with similar data recently obtained for the TMA·SO_2,[1] DMA·SO_2,[2] and HCN·SO_2[3] complexes. All four complexes have similar L-shaped conformations with an N···S interaction. Table VI summarizes structural data, dipole moments, quadrupole coupling constants, and estimates of dissociation energies from various sources, including analysis of centrifugal distortion data (see below).

TMA·SO_2 has been widely studied theoretically and experimentally as a prototype amine·SO_2 charge-transfer complex. It is the only complex whose dissociation energy in the gas phase is experimentally known (9.1 kcal/mol). The nitrogen to sulfur distance in Py·SO_2 of 2.61 Å is significantly longer than in TMA·SO_2 (2.26 Å) and DMA·SO_2 (2.34 Å), but shorter than in HCN·SO_2 (2.98 Å) and much shorter than the sum of the N–S van der Waals radii (3.35 Å).[25] This trend in N···S distances correlates with the increase in ionization potential for the nitrogen species (Table VI). The correlation with their gas-phase proton affinities is less regular except that HCN is obviously not comparable to the three bases.

The L-shaped conformation of the complexes suggests a n–π^* interaction as the driving force for the association. However, Douglas and Kollman[26] pointed out for TMA and DMA that the electrostatic interaction is the largest attractive energetic term, with polarization and charge transfer somewhat smaller. Using a Morokuma[27] energy decomposition analysis, they obtained ΔE_{ES}:ΔE_{POL}:ΔE_{CT} in the ratio (kcal/mol) 31.8:4.9:14.1 for TMA·SO_2. This has been discussed more thoroughly elsewhere.[28] It seems clear from the short N···S distances for the TMA, DMA, and Py complexes that their interactions with SO_2 are somewhat stronger than usually found in weak complexes (especially van der Waals complexes) and that modest amounts of charge transfer appear to markedly affect the interaction distance. The case of HCN·SO_2 seems more ambiguous; the N···S distance is only 0.3–0.4 Å shorter than the sum of the van der Waals radii. The large dipole moment of HCN (2.98 D) could be a significant factor in this slight shortening. Also, a theoretical calculation[29] has concluded that transfer of only 0.01 e^- occurs in HCN·SO_2.[30]

Table VII. Ab Initio Structural Parameters and Dissociation Energies for Pyridine·SO_2 Complex[a]

	HF/3-21G	HF/3-21G*[b]	HF/6-31G
	L-Shaped Structure[c,d]		
d(N–S) (Å)	2.48	2.39	2.55
α (deg)	2.4	1.6	3.0
β (deg)	87	84	84
ΔE_{diss} (kcal·mol^{-1})	13.3	12.6	11.4
	Staggered Structure[c,e]		
d(N–S) (Å)	2.65	2.58	2.67
α (deg)	12	11	8
β (deg)	89	85	85
ΔE_{diss} (kcal·mol^{-1})	10.6	9.9	9.4
E_{SCF}(pyridine)	−245.3105	−245.3105	−246.5927
E_{SCF}(SO_2)	−544.2463	−544.5033	−546.9034

[a] Pyridine and SO_2 geometries fixed.[18,19] [b] Same basis set as 3-21G except sulfur atom has five d polarization functions. [c] See Figure 1 for definition. [d] Experimental conformation, Figure 1A. [e] Figure 1B.

The dipole moments of the complexes, as well as the estimated induced dipole moments, also suggest a decrease in the interaction with SO_2 in going from TMA to Py (Table VI), which parallels the N···S distances. The dipole moment of Py·SO_2 indicates a fairly large induced dipole moment for this complex compared to some other complexes with sulfur dioxide such as ethylene·SO_2[23] or $H_2O{\cdot}SO_2$.[24] The vector sum of the nearly orthogonal dipole moments of free SO_2 (1.633 D)[22] and pyridine (2.23 D)[32] predicts dipole components of μ_a = 2.40, μ_c = 1.13, and μ_{total} = 2.65 D for the complex. The difference between these and the observed values gives an induced dipole moment of μ_a = 1.96, μ_c = 0.18, and μ_{ind} = 1.97 D. This induced moment is nearly aligned with the N–S bond vector. Since there is likely to be some charge transfer from nitrogen to sulfur on the basis of the short N···S distance, an upper limit is estimated for this effect by assuming that the induced moments arise only from the charge-transfer term. This gives a transfer of 0.15 e^- from nitrogen to sulfur, which can be compared with the TMA·SO_2 and DMA·SO_2 complexes where a similar analysis gave μ_{ind} = 3.49 and 2.78 D and an upper limit of 0.32 and 0.25 e^-, respectively. Since this interpretation ignores any vibrational effects and other polarization effects, the actual charge transfer cannot be established.

The ^{14}N nuclear quadrupole coupling constants are also perturbed in a regular manner upon complexation. The coupling constant χ_{aa} samples the electronic environment along the a inertial axis at the nitrogen; this axis is within 3° of the N–S bond vector. The quantity $\Delta\chi_{aa}$ (Table VI) is the difference between the expected value based on the free monomer and the value in the complex. The $\Delta\chi_{aa}$ values imply that the perturbations of the electronic environment are greatest in TMA·SO_2 and decrease regularly to HCN·SO_2. A more quantitative interpretation of this quantity is complex and has been explored for the TMA·SO_2 complex.[1]

Another indication of the relative strength of the complexes can be obtained from the pseudodiatomic stretching force constant for the complexes. They provide an estimate for the force constant for stretching the complex along the R_{cm} coordinate. These are obtained from D_J[33] (Table II). They can be used to estimate the vibrational frequency and the amplitude of vibration for the stretching mode ($\langle\Delta R_{cm}{}^2\rangle^{1/2}$) assuming a harmonic vibration. The well depth ϵ can be estimated for a Lennard-Jones 6–12 potential using $\epsilon = k_s R_{cm}{}^2/72$. These values are listed in Table VI and vary in a manner that parallels the N···S distance. The trend in the

(22) Muenter, J. S. *J. Chem. Phys.* **1968**, *48*, 4544.
(23) Andrews, A. M.; Taleb-Bendiab, A.; Hillig, K. H., II; Kuczkowski, R. L. *J. Chem. Phys.* **1990**, *93*, 7030.
(24) Matsumura, K.; Lovas, F. J.; Suenram, R. D. *J. Chem. Phys.* **1989**, *91*, 5887.
(25) Pauling, L. *The Nature of the Chemical Bond*, 3rd ed.; Cornell University Press: Ithaca, NY, 1960; Chapter 7.
(26) Douglas, J. E.; Kollman, P. A. *J. Am. Chem. Soc.* **1978**, *100*, 5226.
(27) Morokuma, K. *Acc. Chem. Res.* **1977**, *10*, 294.
(28) (a) Kollman, P. A. *Acc. Chem. Res.* **1977**, *10*, 365. (b) Kollman, P. A. *J. Am. Chem. Soc.* **1977**, *99*, 4875. (c) Douglas, J. E.; Kollman, P. A. *J. Am. Chem. Soc.* **1980**, *102*, 4293. (d) Kollman, P. A. *J. Am. Chem. Soc.* **1978**, *100*, 2974.
(29) Chattopadhyay, S.; Moore Plummer, P. L. *J. Chem. Phys.* **1990**, *93*, 4187.
(30) For comparison, Δq_{SO_2} (increased Mulliken population) in the TMA·SO_2 complex was 0.15–0.17.[31]
(31) (a) Sakaki, S.; Sata, H.; Imai, Y.; Morokuma, K.; Ohkubo, K. *Inorg. Chem.* **1985**, *24*, 4538. (b) Pradeep, T.; Sreekanth, C. S.; Hegde, M. S.; Rao, C. N. R. *J. Am. Chem. Soc.* **1989**, *111*, 5058.
(32) Nelson, R. D.; Lide, D. R.; Maryott, A. A. *NSRDS-NBS* **1967**, *10*.
(33) Millen, D. J. *Can. J. Chem.* **1985**, *63*, 1477.

well depth ϵ clearly signifies a steady decrease from $TMA{\cdot}SO_2$ to $HCN{\cdot}SO_2$. Nevertheless, the absolute values for ϵ are certainly unreliable, at least for the stronger complexes. This procedure underestimates ΔE_{diss} for $TMA{\cdot}SO_2$ by 5.2 kcal/mol.[1]

As a final measure of the relative stabilities of the two different conformations of pyridine relative to the SO_2 plane (Figure 1) as well as the relative strengths of the adducts from $TMA{\cdot}SO_2$ to $HCN{\cdot}SO_2$, ab initio calculations (HF/SCF) were examined. A growing body of work indicates that the relative stabilities of various conformations can be estimated at the HF level although structural details and binding energies will be unreliable in an absolute sense. The structural parameters for the two different conformers (Figure 1) were optimized by using GAUSSIAN86[34] with three different basis sets. The results are given in Table VII. Indeed, the ab initio results favor the experimental conformation by 2-2.5 kcal/mol. Simple electrostatic energy calculations were also carried out for the two conformations using the distributed multipole model of Buckingham and Fowler.[35] The multipole moments for the atoms in pyridine and SO_2 were obtained from the literature.[35,36] The electrostatic interaction energy was calculated at the experimental N···S separation for the two conformations; this also favored the experimental conformation by about 2 kcal/mol. This conformation is consistent with the quadrupole moments for SO_2[37] and pyridine,[38] providing a simple rationale for the observed result.

The optimized calculations at the HF/3-21G* level for $TMA{\cdot}SO_2$, $DMA{\cdot}SO_2$, $Py{\cdot}SO_2$, and $HCN{\cdot}SO_2$ can also be compared. The calculated ΔE_{diss} for this series varies in a regular fashion (kcal/mol): 17.2, 16.6, 12.6, and 3.34 (Table VI).

We conclude from this evidence that this series represents a transition from a complex with a modest charge-transfer interaction ($TMA{\cdot}SO_2$) to one with virtually none in $HCN{\cdot}SO_2$. The dissociation energies decrease from 9.1 kcal/mol (experimental)[8] in $TMA{\cdot}SO_2$ to roughly 1-3 kcal/mol in $HCN{\cdot}SO_2$[29] while d(N···S) increases by 0.7-0.8 Å. Thus, relatively small changes in the stabilities and the amounts of charge transfer have rather pronounced geometric effects for these complexes.

Acknowledgment. We are grateful to the donors of the Petroleum Research Fund, administered by the American Chemical Society, for support of this work. The research was also supported by the National Science Foundation, Washington, DC.

Registry No. $C_5H_5N{\cdot}SO_2$, 21326-53-4; $C_5H_5{}^{15}N{\cdot}SO_2$, 135639-37-1; $C_5D_5N{\cdot}SO_2$, 135639-38-2; $C_5H_5N{\cdot}S^{18}O_2$, 135639-39-3; $C_5H_5N{\cdot}{}^{34}SO_2$, 135639-40-6.

Supplementary Material Available: Tables S1-S6 listing observed and calculated transition frequencies and Stark effect data (6 pages). Ordering information is given on any current masthead page.

(34) Frisch, M. J.; Binkley, J. S.; Schlegel, H. B.; Raghavachari, K.; Melius, S. F.; Martin, R. L.; Stewart, J. J. P.; Bobrowicz, F. W.; Rohlfing, C. M.; Kahn, L. R.; DeFrees, D. J.; Seeger, R.; Whiteside, R. A.; Fox, D. J.; Fluder, E. M.; Pople, J. A. *GAUSSIAN86*; Carnegie-Mellon Quantum Chemistry Publishing Unit: Pittsburgh, PA, 1986.
(35) (a) Buckingham, A. D.; Fowler, P. W. *J. Chem. Phys.* **1983**, *79*, 6426. (b) Buckingham, A. D.; Fowler, P. W. *Can. J. Chem.* **1985**, *63*, 1918.
(36) Price, S. L.; Stone, A. J. *Chem. Phys. Lett.* **1983**, *98* (5), 419.
(37) Pochan, J. M.; Stone, R. G.; Flygare, W. H. *J. Chem. Phys.* **1969**, *51*, 4278.
(38) Harver, E.; Sutter, D. H. *Z. Naturforsch.* **1976**, *31a*, 266.
(39) Kimura, K.; Katsumata, S.; Achiba, Y.; Yamazaki, T.; Iwata, S. *Handbook of Hel Photoelectron Spectra of Fundamental Organic Molecules*; Halsted Press: New York, 1981.
(40) (a) Staley, R. H.; Taagepera, M.; Henderson, W. G.; Koppel, I.; Beauchamp, J. L.; Taft, R. W. *J. Am. Chem. Soc.* **1977**, *99*, 326. (b) Staley, R. H.; Kleckner, J. E.; Beauchamp, J. L. *J. Am. Chem. Soc.* **1976**, *98*, 2081. (c) Kollman, P.; Rothenberg, S. *J. Am. Chem. Soc.* **1977**, *99*, 1333.

Newly Designed Permanganate-Reductant Chemical Oscillators[1]

Christopher J. Doona,[†] Kenneth Kustin,[†] Miklós Orbán,*[,#] and Irving R. Epstein*[,†]

Contribution from the Department of Chemistry, Brandeis University, Waltham, Massachusetts 02254-9110, and Institute of Inorganic and Analytical Chemistry, L. Eötvös University, P.O. Box 32, H-1518, Budapest 112, Hungary. *Received April 15, 1991*

Abstract: The subfamily of manganese oscillating chemical reactions containing permanganate as oxidant, plus a reductant, and phosphate to stabilize intermediate Mn oxidation states has been expanded in two ways. The "minimal" manganese oscillator, $MnO_4^- + Mn^{2+} + H_2PO_4^-$, and several of its oscillatory derivatives give oscillation when either arsenate or vanadate replaces phosphate. Oscillatory behavior in a flow reactor has also been found for seven new reductants: arsenite, thiocyanate, thiourea, ascorbic acid, hydroxylamine, dithionite, and nitrite. A two-component permanganate oscillator is constructed using arsenite as the reductant, in which the stabilizing arsenate is generated as a reaction product. Our results yield insight into the roles of the reductant and the stabilizer in promoting oscillation.

The systematic design of chemical oscillators, after having initially focused on halogen chemistry, has progressed through other regions of the periodic table and now includes a family of oscillating reactions based on the chemistry of the transition metal manganese.[2-6] The oscillatory core is the Guyard reaction ($MnO_4^- + Mn^{2+}$)[7] with the addition of dihydrogen phosphate (hereafter referred to as phosphate) performed under flow conditions in a continuously stirred tank reactor (CSTR). This family of oscillators is divided into two subfamilies; the first consists of permanganate and a reductant, and the second consists of manganese(II) and an oxidant.

[†] Brandeis University.
[#] L. Eötvös University.

(1) Part 74 in the series: Systematic Design of Chemical Oscillators. Part 73: Wang, R. T.; Rábai, G.; Kustin, K. *Int. J. Chem. Kinet.*, in press.
(2) Nagy, A.; Treindl, L. *Nature* **1986**, *320*, 344.
(3) Fazekas, T.; Mrakavova, M.; Nagy, A.; Olexova, A.; Treindl, L. *React. Kinet. Catal. Lett.* **1990**, *42*, 181.
(4) Orbán, M.; Epstein, I. R. *J. Am. Chem. Soc.* **1989**, *111*, 8543.
(5) Orbán, M.; Epstein, I. R. *J. Am. Chem. Soc.* **1990**, *112*, 1812.
(6) Orbán, M.; Lengyel, I.; Epstein, I. R. *J. Am. Chem. Soc.* **1991**, *113*, 1978.
(7) Guyard, G. *Bull. Soc. Chim. Fr.* **1864**, *1*, 89.

0002-7863/91/1513-7484$02.50/0